Impact of an intense water column mixing (0-1500 m) on prokaryotic diversity and activities during an open-ocean convection event in the NW Mediterranean Sea

Tatiana Severin, Caroline Sauret, Mehdi Boutrif, Thomas Duhaut, Fayçal Kessouri, Louise Oriol, Jocelyne Caparros, Mireille Pujo-Pay, Xavier Durrieu de Madron, Marc Garel, et al.

environmental microbiology

Environmental Microbiology (2016) **18**(12), 4378–4390 doi:10.1111/1462-2920.13324

Impact of an intense water column mixing (0–1500 m) on prokaryotic diversity and activities during an open-ocean convection event in the NW Mediterranean Sea

Tatiana Severin,[1,2] Caroline Sauret,[1,2] Mehdi Boutrif,[3,4] Thomas Duhaut,[5] Fayçal Kessouri,[5] Louise Oriol,[1,2] Jocelyne Caparros,[1,2] Mireille Pujo-Pay,[1,2] Xavier Durrieu de Madron,[6] Marc Garel,[3,4] Christian Tamburini,[3,4] Pascal Conan[1,2] and Jean-François Ghiglione[1,2]*

[1]*Sorbonne Universités, UPMC Univ Paris 06, UMR 7621, Laboratoire d'Océanographie Microbienne, Observatoire Océanologique, F-66650, Banyuls/mer, France.*

[2]*CNRS, UMR 7621, Laboratoire d'Océanographie Microbienne, Observatoire Océanologique, F-66650, Banyuls/mer, France.*

[3]*Aix-Marseille Université, CNRS, Université de Toulon, IRD, MIO UM 110, 13288, Marseille, France.*

[4]*Université du Sud Toulon-Var, Mediterranean Institute of Oceanography (MIO), 83957, La Garde Cedex, France CNRS-INSU/IRD UM 110.*

[5]*LA, CNRS, Université de Toulouse, 14 avenue Edouard Belin, 31400 Toulouse, France.*

[6]*CEFREM, UMR 5110, CNRS-UPVD, F-66860, Perpignan, France.*

Summary

Open-ocean convection is a fundamental process for thermohaline circulation and biogeochemical cycles that causes spectacular mixing of the water column. Here, we tested how much the depth-stratified prokaryotic communities were influenced by such an event, and also by the following re-stratification. The deep convection event (0–1500 m) that occurred in winter 2010–2011 in the NW Mediterranean Sea resulted in a homogenization of the prokaryotic communities over the entire convective cell, resulting in the predominance of typical surface Bacteria, such as *Oceanospirillale* and *Flavobacteriales*. Statistical analysis together with numerical simulation of vertical homogenization evidenced that physical turbulence only was not enough to explain the new distribution of the communities, but acted in synergy with other parameters such as exported particulate and dissolved organic matters. The convection also stimulated prokaryotic abundance (+21%) and heterotrophic production (+43%) over the 0–1500 m convective cell, and resulted in a decline of cell-specific extracellular enzymatic activities (−67%), thus suggesting an intensification of the labile organic matter turnover during the event. The rapid re-stratification of the prokaryotic diversity and activities in the intermediate layer 5 days after the intense mixing indicated a marked resilience of the communities, apart from the residual deep mixed water patch.

*For correspondence. E-mail ghiglione@obs-banyuls.fr; Tel. +33 (0) 4 68 88 73 16; Fax +33 (0) 4 68 88 73 98.

Introduction

Deep open-ocean convection is an essential process for the thermohaline circulation of the global ocean (Marshall and Schott, 1999). In the NW Mediterranean (NWM), this process is responsible for the formation and circulation of the Western Mediterranean Deep Water (WMDW) over the entire western basin (Millot, 1999). Open-ocean convection is an annual event in the Gulf of Lion, triggered by the production of dense surface waters in winter through atmospheric forcing where the 'convection chimney' can reach over 100 km in diameter (Send and Marshall, 1995). During the mixing phase, kilometer scale dense water plumes can sink down to large depth with downward currents exceeding 10 cm s^{-1} (Schott and Leaman, 1991). This sinking flow is balanced by upward motions of deep waters enriched in nutrients, which sustain the spring phytoplanktonic bloom occurring in NWM (Severin *et al.*, 2014). Particulate and dissolved organic carbon (POC and DOC) exported to deep waters have the potential to enhance deep-sea biological activities (Tamburini *et al.*, 2013a; Martini *et al.*, 2014). Open-ocean convection indirectly contributes to the carbon sequestration by stimulating the biological carbon pump, but also by enhancing the export of POC (~10 mg C m^{-2} d^{-1}; Stabholz *et al.*, 2013), and DOC (~3000 mg C m^{-2} d^{-1};

Santinelli *et al*., 2010). The quantity and the quality of the exported organic matter may have important consequences for the diversity and activity of heterotrophic prokaryotes (Bacteria and Archaea).

In oligotrophic regions such as the Mediterranean Sea, the functioning and productivity of the pelagic ecosystem largely depends on the activity of heterotrophic prokaryotes, which are responsible for the balance between exported and mineralized carbon (Pulido-Villena *et al*., 2012). In the euphotic zone, prokaryotes are abundant, reaching abundances of around 10^6 cells ml^{-1} and consume 20–50% of the daily primary production (Ducklow, 1999). Below the deep chlorophyll maximum, prokaryotic abundance and heterotrophic production decreases exponentially with depth (Tanaka and Rassoulzadegan, 2004). In previous studies, a stable vertical zonation of bacterial community structure was observed at several offshore stations and at different seasons in the Mediterranean Sea, with a clear stratification in three layers: above the deep chlorophyll maximum (DCM), in the DCM and deeper (Ghiglione *et al*., 2007; 2008; 2009; Rodríguez-Blanco *et al*., 2009). Archaeal communities also appeared to be highly stratified between the surface and meso- and bathypelagic waters in the Mediterranean Sea (De Corte *et al*., 2009; Tamburini *et al*., 2009; Winter *et al*., 2009).

Few studies have had the opportunity to evaluate the response of the prokaryotic community to intense mixing of the water column caused by open-ocean convection. In the Southern Adriatic Sea, an increase of prokaryote abundance and activity was observed in the deep water masses following open-ocean deep convection and dense shelf water cascading episodes (Azzaro *et al*., 2012). Similar increases were found during intermediate convection events ($\sim$300 m) in the Sargasso Sea and in the Adriatic Sea, but contradictory results were found on their impact on prokaryotic diversity (Morris *et al*., 2005, Najdek *et al*., 2014).

The purpose of this study was to test the impact of deep mixing on the dynamic of stratified prokaryotic communities. We investigated a deep convection event (0–1500 m) and tested whether the physical turbulence alone or combined with other biogeochemical parameters could explain the structure of the prokaryotic communities during the convection event. We further examine how such an event impacted prokaryotic abundance, heterotrophic production and extracellular enzymatic activities. In addition, we investigated the resilience of the prokaryote diversity and activities in the surface, intermediate and deep layers 5 days after the cessation of the convective vertical currents.

Results

Hydrography

Three hydrological conditions have been studied according to the temperature and salinity properties of the water column at the sampled stations (Fig. 1). At station ANTARES (ANT; Fig. 1B), 3 major water masses were observed: the Atlantic Waters (AW) between 0 and 250 m depth, dispersed in potential temperature (13.1–13.4°C) and salinity (38.1–38.4); the warmer (13.3°C) and saltier (38.5) Levantine Intermediate Waters (LIW) from 250 to 600 m; and the coldest (12.9°C), saltiest (38.4) and densest (potential density anomaly $>$ 29.1 kg m^{-3}) WMDW situated from 600 m to the bottom (2500 m). The presence of the three typical NW Mediterranean water masses at ANT illustrated that this station situated outside of the convection area was well stratified and not impacted by the convective mixing, as described in Severin and colleagues (2014). ANT is then used as a reference station for the further analyses and discussions. The convective mixing was clearly observed at the SC station (SCC) (Fig. 1C) with a homogeneous cold (12.9°C), salty (38.4), and dense ($>$29.1 kg m^{-3}) water mass in the upper 1500 m of the water column, indicative of a deep convective mixed layer. The colder (12.9°C) and saltier (38.5) underneath layer was mostly composed of recent deep waters formed during an episode of bottom-reaching convection that occurred at the same location one month before our sampling (Severin *et al*., 2014). The same station sampled 5 days after the convection episode (SCS) was characterized by the reappearance of a re-stratified water column organized in three water masses (Fig. 1D): AW (12.8°C, 38.3) in the upper tens of meters of the water column, LIW (13.2°C, 38.5) between 100 and 500 m deep, and newly-formed WMDW (12.9°C, 38.4) composed of the WMDW around 2000 m formed by the convection episode of February (noted $nWMDW_{feb}$), and the WMDW around 1000 m formed by the convection of March (noted $nWMDW_{mar}$).

Prokaryotic community structures

Bacterial community structures mostly followed the distribution of the corresponding water masses (Fig. 2). At the stratified stations (ANT and SCS), communities of each water mass clustered together and independently of the station except the community in SCS at 10 and 50 m which clustered with the convection community (SCC) while they were sampled in the AW (Fig. 1D). Significant dissimilarities were found between the surface (AW) and the deep layers (LIW and WMDW) (ANOSIM $R = 0.80$, $P < 0.01$) and between LIW and WMDW, (ANOSIM $R = 0.99$, $P < 0.01$). During the convection event (SCC), the bacterial community structure was homogeneous throughout the 0–1500 m mixed water layer, and differed for the deepest sample SCC2000m located below the mixing zone. SCC community structure influenced by the convection was significantly different to the ANT community in the AW (ANOSIM $R = 0.91$, $P < 0.05$), but was closer to AW assemblage than LIW and WMDW assemblages.

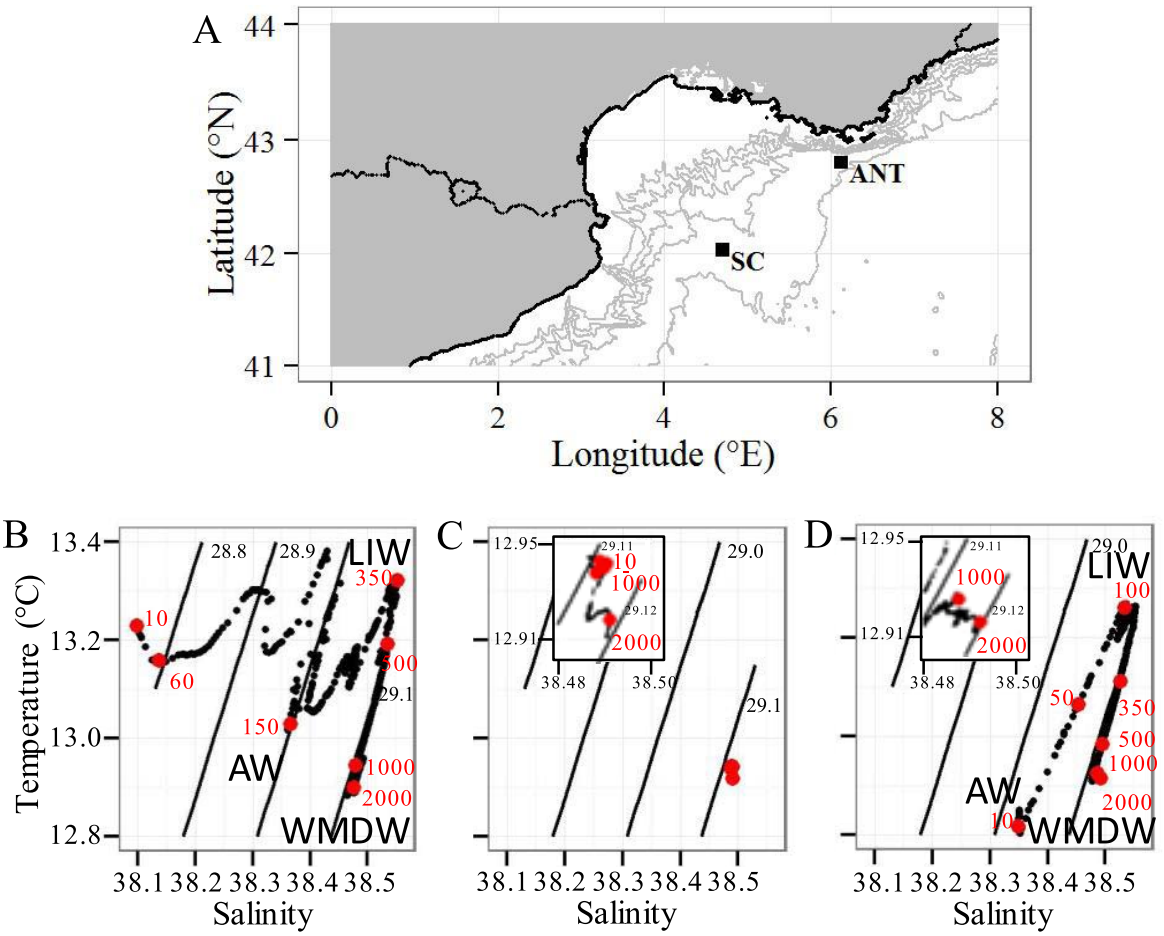

Fig. 1. (A) Map of sample location during the CASCADE cruise leg 1 (1–23 March 2011). Potential Temperature (°C) - salinity diagrams (T-S) at stations (B) ANT, (C) SCC (with a zoom on top-left), and (D) SCS (with a zoom of the WMDW on top-left where the $nWMDW_{mar}$ are observed around 1000 m and the $nWMDW_{feb}$ around 2000 m). The lines and the annotated values in the diagrams represent the potential density anomalies with their values. The sampling depths are indicated as well as the corresponding water masses (AW for Atlantic water, LIW for Levantine Intermediate Water and WMDW for Western Mediterranean Deep Water).

Alphaproteobacteria dominated the bacterial diversity of all the samples (27–49% of all the sequenced bacterial operational taxonomic units; OTUs) (Fig. 3), in which the SAR11 composed the majority of the OTUs of the *Alphaproteobacteria* class (87% of the *Alphaproteobacteria*, and 24–43% of total bacterial OTUs). At the stratified stations (ANT and SCS), SAR11, *Flavobacteriales*, *Oceanospirillales* and *Synechoccocales* represented the most abundant OTUs in the AW with 34–44%, 9–24%, 12–19%, and 3–16% of total bacterial OTUs, respectively, even if SCS10m and SCS50m are closer to the convection community than the AW according to the unweighted-pair group method with arithmetic averages (UPGMA) (Fig. 2). In the LIW and WMDW, the contribution of these taxonomic classes decreased drastically, with the notable absence of *Synechoccocales*. SAR11 remained predominant in the LIW and WMDW with 32–42% and 32–36%, of the total bacterial community respectively. Some OTUs were undetected at the surface layers but were identified in the deeper water mass (WMDW), such as SAR406 (10–18% and 9–16% in the LIW and WMDW, respectively), Sva0853 from *Deltaproteobacteria* (2–6%, 3–7% in the LIW and WMDW, respectively), and SAR202 (2–3%, 5–8% in the LIW and WMDW, respectively).

Overall, convective communities were dominated by taxa found in surface stratified waters. For example, SAR11 (from 25 to 33% of total bacterial OTUs), *Oceanospirillales* (from 16 to 29% of total bacterial OTUs) and *Flavobacteriales* (from 19 to 22% of the total bacterial community) dominated the convective community and were mainly found in surface waters under the stratified regime. OTUs overwhelmingly found in deep stratified waters were also found but in lower abundance in convective waters, such as SAR406 (4–6% of total bacterial OTUs) and SAR202 (from 0.5 to 1% of total bacterial OTUs). The bacterial diversity at SCC2000m and

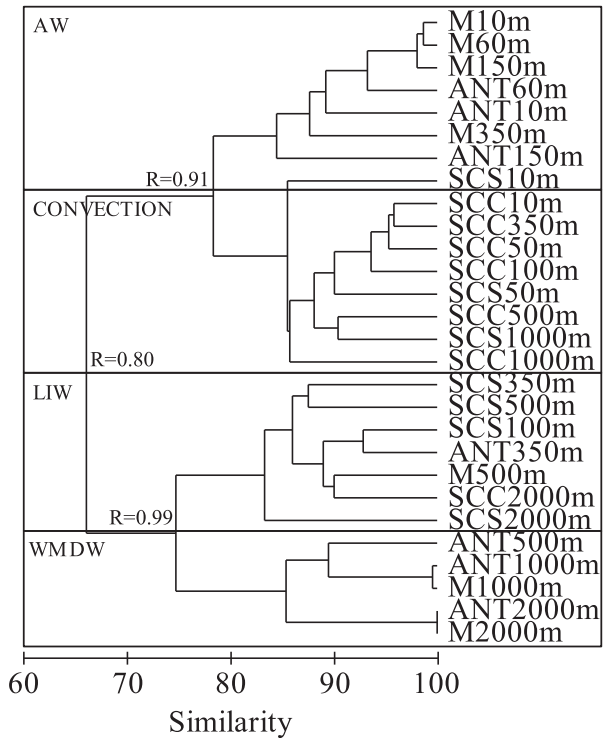

Fig. 2. Unweighted-pair group method with arithmetic mean (UPGMA) dendrograms based on Bray-Curtis similarities of 16S rRNA gene bacterial reads from ANT (stratified reference station), SCC (convective station) and SCS (restratified station) sampled at different depths and for the numerical models M Results of ANOSIM tests (R) are indicated at the main nodes. Samples clustering in the same water masses (AW, LIW and WMDW) are indicated by rectangles.

SCS2000m was slightly different compared with the corresponding WMDW diversity at ANT2000m with higher abundance of *Flavobacteriales* (+84%), *Oceanospirillales* (+70%) and *Acidimicrobiales* (+75%) to the expense of SAR406 (−18%), Sva0853 (−50%); SAR202 (−60%) and *Thiohalorhabdales* (−44%).

In the stratified stations (ANT and SCS), we found a higher bacterial richness and evenness (Supporting Information Table S1) in the deep WMDW (Chao1 = 142 ± 21, Pielou = 0.74 ± 0.02) than in the surface AW (Chao1 = 107 ± 12, Pielou = 0.62 ± 0.01). As for the WMDW, LIW had an elevated richness and evenness (Chao1 = 138 ± 28, Pielou = 0.73 ± 0.03) than in the AW. Values of the convective bacterial diversity indexes (SCC) were between AW and LIW indexes (Chao1 = 134 ± 21, Pielou = 0.66 ± 0.01).

Environmental drivers of the prokaryotic community structures

To investigate the influence of pure physical water mixing on the bacterial community structures, we constrained the OTU table obtained at the reference station ANT by applying a modified SYMPHONIE model. This model simulates the transport of particles in the water column during the 5 days of the convection event simulated by the MERCATOR global model for the ocean circulation. The numerical simulation showed that physical mixing alone was not sufficient to explain the changes in bacterial community structure observed during the convective event in SCC samples. Indeed, the numerically simulated convective bacterial community structures (M) did not result in a grouping within a 'convective' cluster as it happened for SCC samples, but rather stayed similar to the natural assemblages at the stratified reference station ANT organized in 3 clusters according to the three waters masses AW, LIW and WMDW (Fig. 2). In the same way, the numerical simulation resulted in similar proportion of taxa in each water masses compared with the stratified stations ANT and SCS (Fig. 3). The numerically simulated M communities in the AW water mass were dominated by SAR11 (39%), *Flavobacteriales* (14%), *Oceanospirillales* (12%) and *Synechoccocales* (11%). Like the natural bacterial communities in ANT and SCS, *Flavobacteriales*, *Oceanospirillales* and *Synechoccocales* decreased in the numerically simulated communities M in the LIW and WMDW, while the deep OTUs (SAR 406, Sva0853 and SAR202) increased.

We further explored the environmental drivers of the bacterial community structures at the reference station (ANT), as well as during (SCC) and after (SCS) the convective event (Fig. 4). Prior to the direct statistical multivariate canonical correspondence analysis (CCA) analyses, Spearman's rank pairwise correlation tests were calculated between environmental variables at each station. As the presence of correlated variables in the same CCA would lead to superimposed arrows, only one variable was selected and the covariables were removed from the analysis (i.e. 'partialled out') to get a clearer picture (Ter Braak *et al.*, 2002). The use of one variable instead of several covariables would not significantly change the explained variance of the species-environment relationship of the CCA (Ter Braak *et al.*, 2002). A summary of the correlated variables and the corresponding selected variable for the CCA analyses is presented in the supplementary information (Supporting Information Table S2). For the ANT station, strong correlation was found between nitrate (NO_3+NO_2), phosphate (PO_4), silicate ($Si(OH)_4$), salinity and density ($R > 0.90$, $P < 0.01$, $n = 7$). Nitrate was then selected for the CCA analysis at ANT, and used as representative variable for PO_4, $Si(OH)_4$, salinity and density (Supporting Information Table S2). For the CCA at the SCC station, the chlorophyll *a* (Chla) was selected and used as representative variable for POP and phaeopigments *a* (Phaeo *a*) ($\rho > 0.90$, $P < 0.01$, $n = 7$). The same approach was used for station SCS ($\rho > 0.90$, $P < 0.01$,

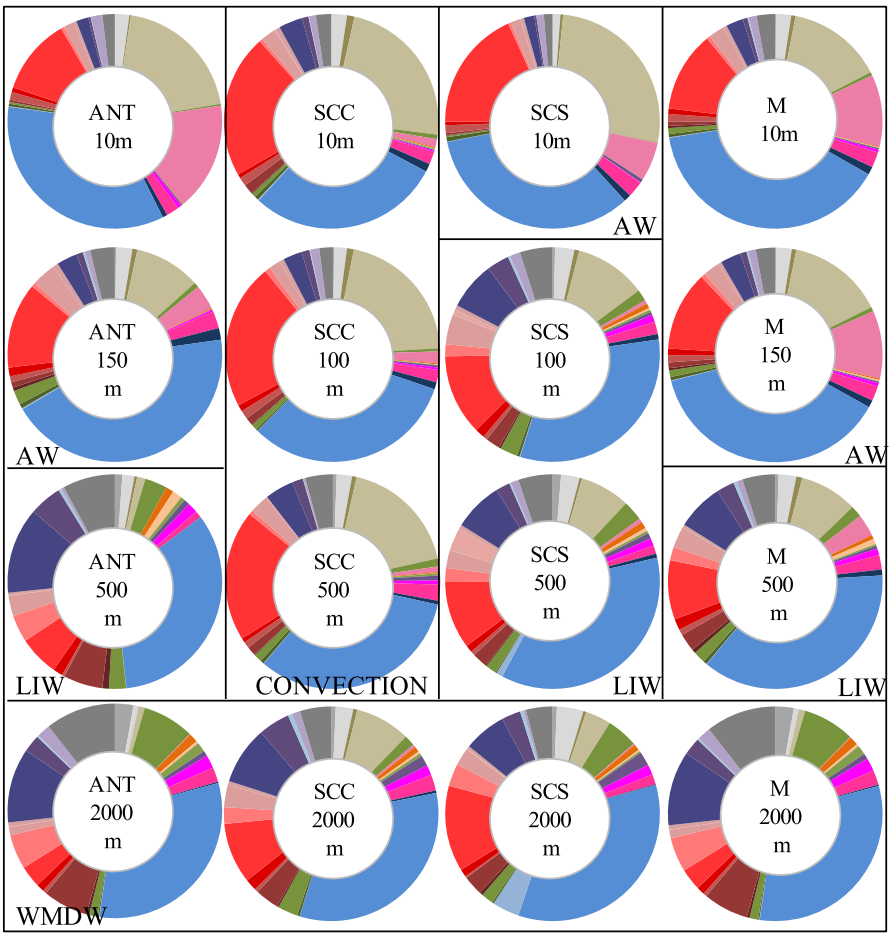

- Acidobacteria__Acidobacteria-6__iii1-15
- Bacteroidetes__Cytophagia__Cytophagales
- Chloroflexi__SAR202__NA
- Gemmatimonadetes__Gemm-2__NA
- PAUC34f__NA__NA
- Planctomycetes__Planctomycetia__Pirellulales
- Proteobacteria__Alphaproteobacteria__Rhodobacterales
- Proteobacteria__Betaproteobacteria__Burkholderiales
- Proteobacteria__Deltaproteobacteria__Desulfobacterales
- Proteobacteria__Deltaproteobacteria__Sva0853
- Proteobacteria__Gammaproteobacteria__NA
- Proteobacteria__Gammaproteobacteria__Thiohalorhabdales
- Proteobacteria__Gammaproteobacteria__Vibrionales
- SAR406__AB16__Arctic96B-7
- Verrucomicrobia__[Pedosphaerae]__Arctic97B-4
- Others (less than 1%)
- Actinobacteria__Acidimicrobiia__Acidimicrobiales
- Bacteroidetes__Flavobacteriia__Flavobacteriales
- Cyanobacteria__Synechococcophycideae__Synechococcales
- Nitrospirae__Nitrospira__Nitrospirales
- Planctomycetes__Phycisphaerae__Phycisphaerales
- Proteobacteria__Alphaproteobacteria__NA
- Proteobacteria__Alphaproteobacteria__SAR11
- Proteobacteria__Betaproteobacteria__Methylophilales
- Proteobacteria__Deltaproteobacteria__Myxococcales
- Proteobacteria__Gammaproteobacteria__Alteromonadales
- Proteobacteria__Gammaproteobacteria__Oceanospirillales
- Proteobacteria__Gammaproteobacteria__Thiotrichales
- Proteobacteria__NA__NA
- SAR406__AB16__ZA3648c
- Bacteria__NA__NA__NA

Fig. 3. Bacteria taxonomic distribution (Phylum_Class_Order) for OTUs that occurred more than 34 times (> 1% of randomly re-sampled 3372 sequences reads at a clustering distance of 0.03) in the original OTU table and in the numerical models (M10m to M2000m). The remaining sequences are grouped in « other ». Taxonomy not assigned, NA. Samples from the same water masses (AW, LIW and WMDW) are indicated by rectangles.

n=7), which resulted in the use of NO_3+NO_2 for the CCA analysis and used as representative variable for PO_4, Chla, POP and density, and DOP as representative variable for $Si(OH)_4$. For each hydrological regime (ANT, SCC, SCS), four parameters were then selected which explain more than 80% of the changes in the community structure.

The first and second canonical axes explained, respectively, more than 50% and 10% of the variance of the species-environment relationship at each station (Supporting Information Table S3). Others axes accounted each for less than 10% of the variance were not further considered here. At the ANT station the first canonical axis was highly

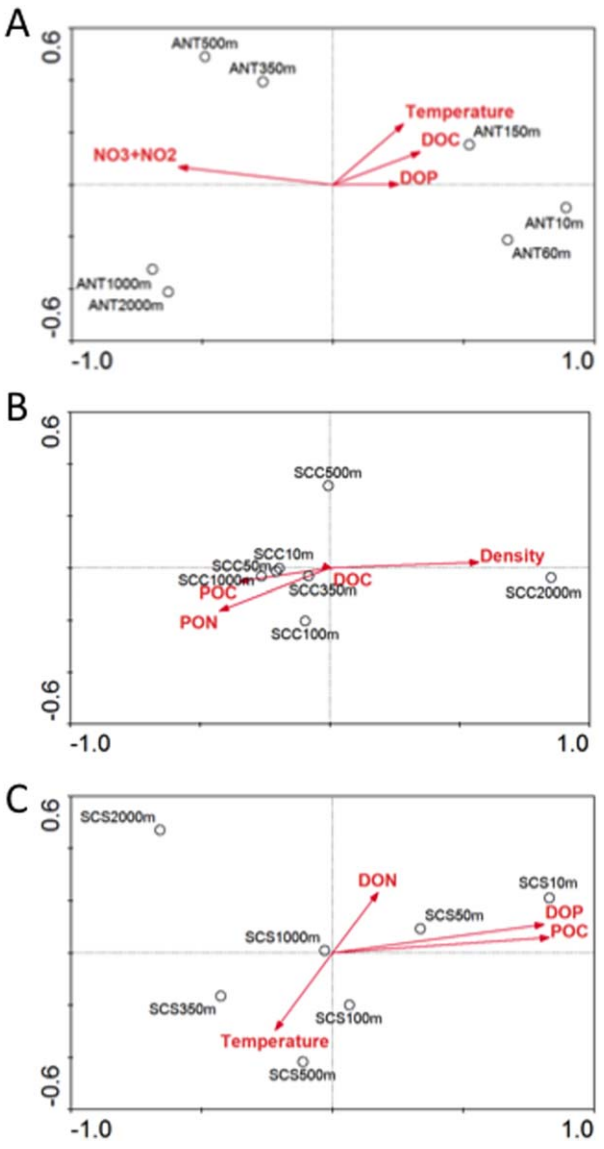

Fig. 4. Canonical correspondence analysis (CCAs) of bacterial community structure at each sampled station: ANT the stratified reference station (A), SCC the convective station (B), SCS the restratified station (C). Arrows point in the direction of increasing values of each variable. The length of the arrows represents degree of correlation with the 2 first axes. NO_3+NO_2: nitrate + nitrite. DOC: dissolved organic carbon. DOP: dissolved organic phosphorus. DON: dissolved organic nitrogen. POC: particulate organic carbon. PON: particulate organic nitrogen.

positively correlated with temperature, DOP, and DOC for bacteria, and negatively correlated with NO_3+NO_2 (and PO_4, $Si(OH)_4$ and density by correlation) (Fig. 4A). The concomitant effect of these parameters explained 89% of the changes in community structure of Bacteria (ratio between the total inertia and the sum of all eigenvalues; Supporting Information Table S3). This implies that the surface bacterial population (10–150 m) is driven by relatively elevated temperature, DOC and POC concentrations, compared with the deeper populations (350–2000 m) driven by high nutrient concentrations in dense waters. At the SCC station, the first canonical axis was positively correlated with density, and negatively correlated with PON and POC. DOC contributed to a lesser extent to the first axis of bacterial community (Fig. 4B). The bacterial population from 10 to 1000 m is then drive by higher DOM and POM than the population at 2000 m living in dense water. All these parameters explained 88% of the changes in community structure of Bacteria (Supporting Information Table S3). At the SCS station, the first canonical axis was highly positively correlated with DOP, DON and POC. The second canonical axis was positively correlated with DON, and negatively with temperature (Fig. 4C). We then return to a more classical repartition with the organic matter that drive the 10–50 m bacterial population, and the 100–1000 m population driven by the relatively high temperature of the LIW (compared with AW and WMDW). Eighty-two percent of the variance was explained by these parameters in the community structure of Bacteria.

Prokaryotic abundances and activities

In the stratified reference station ANT, prokaryotic abundance found in the AW (8.0×10^5 cells ml^{-1} at 10 m) decreased rapidly with depth and stabilized at 5.0×10^4 cells ml^{-1} around 1000 m and below (Fig. 5A). In the convective mixing station (SCC), the prokaryotic abundance was homogeneous between 10 and 1500 m at 2.0×10^5 cells ml^{-1} (SD = 0.41 10^4, $n=7$). Integrated values between 10 and 1500 m were slightly higher at SCC (2.60×10^8 cells m^{-2}) than at ANT (2.05×10^8 cells m^{-2}). In the restratified station (SCS), the prokaryotic abundance throughout the water column was similar to that of the reference station ANT.

Overall, prokaryotic heterotrophic production (PHP) followed the same trend as prokaryotic abundance at the three sampled stations (Fig. 5B). PHP were normalized by the prokaryotic abundance in order to evaluate the cell specific response to the environmental modifications. Elevated production rates were measured in stratified surface waters (4×10^{-5} and 8×10^{-5} ngC l^{-1} h^{-1} $cell^{-1}$ at ANT and SCS, respectively), and progressively decreased to vanish below 500 m depth. PHP was low ($\sim1\times10^{-5}$ ng C l^{-1} h^{-1} $cell^{-1}$) in the convective cell (10–1500 m) but the 10–1500 m integrated production rate was significantly higher in the SCC station (1.32×10^{-2} ngC m^{-2} h^{-1} $cell^{-1}$) than in the ANT station (7.98×10^{-3} ngC m^{-2} h^{-1} $cell^{-1}$; P value <0.05, $n=3$).

At ANT and SCC, PHP were measured in triplicate at *in situ* pressure at 2000 and at 1500 m depth respectively. The pressure effect (Pe), defined as the ratio between PHP obtained under *in situ* pressure and that obtained under decompressed conditions, was calculated to indicate piezophily (adaptation to high pressure) for Pe > 1 and

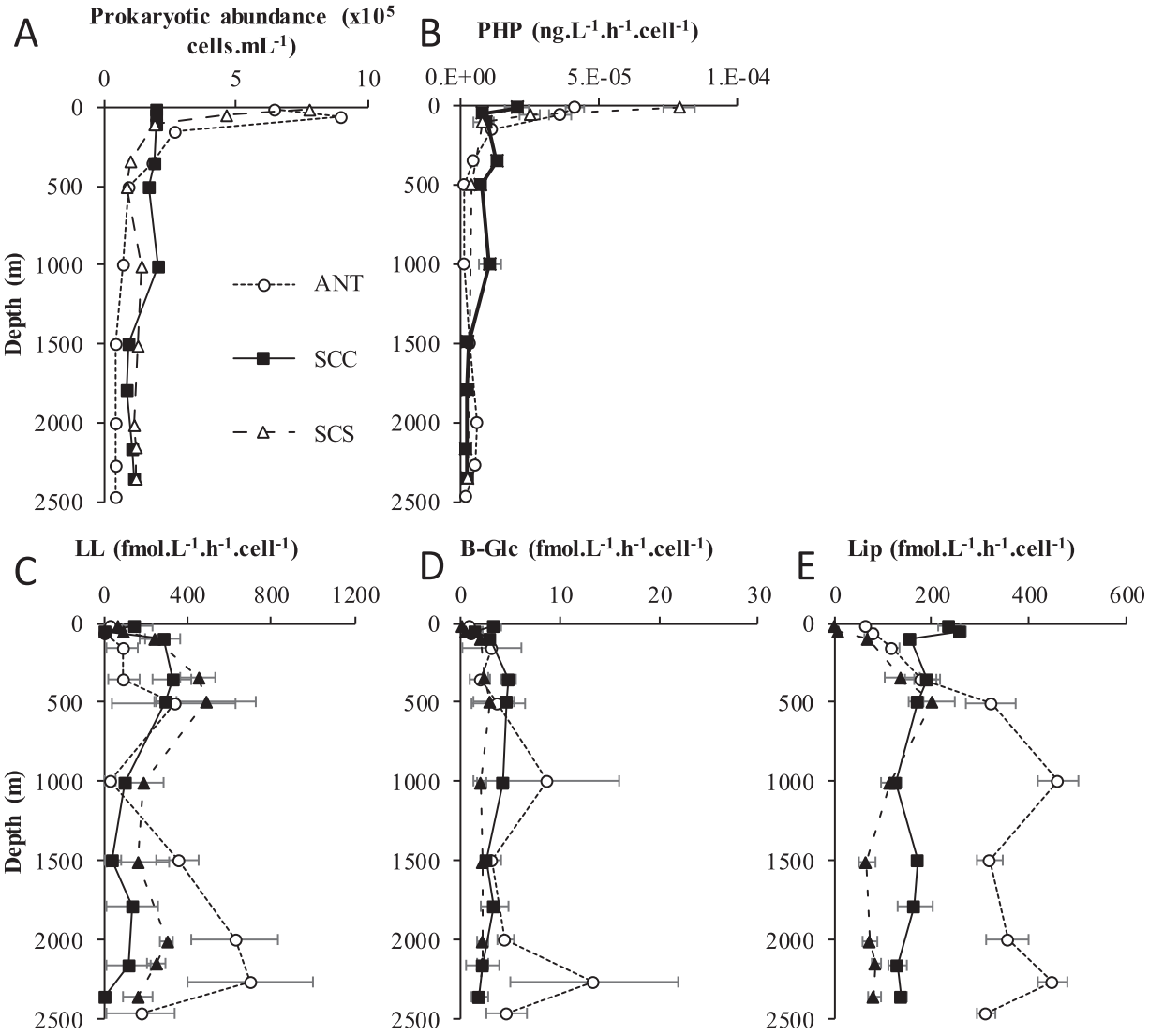

Fig. 5. Vertical changes of (A) prokaryotic abundance, (B) prokaryotic heterotrophic production (PHP) and extracellular (C) aminopeptidase (LL), (D) glucosidase (Glc), and (E) lipase (Lip) activities. Stations ANT (the stratified reference station) in small dashed lines (○), SCC (the convective station) in full line (■), and SCS (the restratified station) in large dashed lines (Δ). For PHP and extracellular activities, the error bars are the standard deviations.

piezosensitivity for $Pe < 1$. The Pe values obtained at 2000 m depth at ANT were significantly higher than 1 ($Pe = 4.7$; P value < 0.05, $n=3$) while those obtained at 1500 m depths at SCC were equal to 1.

Cell specific aminopeptidase (LL), glucosidase (β-Glc) and lipase (Lip) activities were also influenced by the convection event (Fig. 5C–E). At the ANT station, activities were low in the surface (30, 0.8 and 70 fmol l^{-1} h^{-1} $cell^{-1}$ for LL, β-Glc and Lip, respectively), and progressively increases to a maximum activity around 2000 m depth (600, 5 and 400 fmol l^{-1} h^{-1} $cell^{-1}$ for LL, β-Glc and Lip respectively). At the convective station (SCC), activities were quite homogeneous all over the water column and decreased of 67% between 10 and 1000 m compared with ANT. After restratification (SCS station), activities remained low in the surface (0–100 m) and deep layers (below 1000 m), but increased between 100 and 1000 m (maximum values of 3400, 3, 100 and 80 fmol l^{-1} h^{-1} $cell^{-1}$ for LL, β-Glc, Lip and Pho respectively).

Discussion

Effect of open-ocean convection on the vertical prokaryotic community structures

In the stratified reference station ANT situated outside of the convection area, bacterial community was clearly stratified according to the different layers AW, LIW and WMDW. Such vertical stratification seems to be a general

trend in the Mediterranean Sea (Pulido-Villena *et al.*, 2012) and in other oceans (Sunagawa *et al.*, 2015). We also observed an increase in richness (Chao1 of 110 in AW, 100 LIW and >150 in WMDW) and eveness (Pielou of 0.62 in AW, 0.74 in LIW and 0.73 in WMDW) in deeper layers, as previously described (Pommier *et al.*, 2010, Ghiglione *et al.*, 2012). Slight modifications were found in the repartition of prokaryotic taxa with depth, as compared with other studies. In particular, contrary to our study, the deep pelagic habitat of the Mediterranean was previously characterized by higher abundance of *Rhizobiales* (from *Alphaproteobacteria* class), *Oceanospirillales* (*Gammaproteobacteria*), *Desulfuromonadales* (*Deltaproteobacteria*), *Actinobacteridae* (*Actinobacteria*), *Dehalococcoidetes* (*Chloroflexi*), and *Planctomycetacia* (*Planctomycetes*) (Martín-Cuadrado *et al.*, 2007). Despite the elevated relative abundance of *Oceanospirillales* in the deep waters of our study, we found other dominant groups belonging to SAR11 (*Alphaproteobacteria*), Sva0853 (*Deltaproteobacteria*), SAR202 (*Chloroflexi*), and SAR406 in the LIW and WMDW.

The deep convection process resulted in a drastic mixing of the bacterial community structure all over the 0–1500 m convective cell. Previous studies demonstrated that vertical convective currents were able to rapidly export particles from the surface to the deep oceans, with a total mass flux estimated to 90 mg m^{-2} d^{-1} at 1000 m depth (Stabholz *et al.*, 2013). Accordingly, OTUs found in surface waters of the stratified reference station were diluted in the convective cell, as depicted by the typical euphotic *Oceanospirillales* and *Flavobacteriales* that dominated in the entire convective cell (Fig. 3). But the convection process is more complex than a unique export of surface waters to the deep, with upwards currents inside the convective cell that balance out the downward flow (Send and Marshall, 1995). We observed that some typical deep Bacteria (SAR406, SAR202) were carried from the deep to the surface of the convection cell, but in weaker relative abundances compared than the surface taxa exported all over the convective cell. These deep taxa could be transported with the upward currents induced by deep convection event.

In addition, we observed a rapid re-stratification of the upper 500 m within a few days after the convection event (Fig. 1C). The bacterial community assemblage came back to a stratified distribution between 350 and 500 m, with a similar diversity than the LIW of the reference ANT station (Figs. 2 and 3). This phenomenon could be related to the horizontal advection of the LIW over the convection region (Severin *et al.*, 2014). During the re-stratification, the convective vertical currents became null, thus the horizontal advection dominated the surface flow. The LIW brought with them the stratified bacterial community, preventing the Bacteria in the convective chimney to re-colonization their surface habitat. Above 350 m and below 500 m, the bacterial assemblage differs from the usual AW and WMDW communities observed in the stratified reference station (ANT) and remains close to the convective community (Fig. 2). The LIW advection abruptly isolated the AW and trapped a volume of dense mixed water between 500 and 1500 m (named $nWMDW_{Mar}$; Fig. 1D). The $nWMDW_{Mar}$ contained typical surface and deep taxa, an assemblage similar to the convective bacterial community (Figs. 2 and 3). Then the bacterial community formed during the convection survived at least 5 days at 1000 m (SCS1000m) after the convection event. This surface dominant community is susceptible to horizontally spread with the $nWMDW_{Mar}$ in the entire northwestern basin around the depth of $\sim$1000 m during the post-convection propagation phase (Testor and Gascard, 2006). The deeper community at SCS2000m also differed from the other deep communities (Fig 2). This assemblage was present in denser waters formed during a previous bottom-reaching convection event that took place in late January–early February 2011 (named $nWMDW_{Feb}$) (Severin *et al.*, 2014). The observed bacterial assemblage had already been mixed but significantly diverge from the convective community formed in March 2011 and seems to evolve differently than the usual deep community observed in the stratified reference station (ANT, Figs. 2 and 3).

Environmental drivers of prokaryotic community structure

A numerical model was used to simulate the effect of pure physical mixing on the bacterial community distribution along the water column during the convective event. The model was initialized with the OTU table of the stratified communities at the reference station ANT, away from the convection event. The model assumed that Bacteria can be considered as particles with a negligible sinking velocity, and we simulated their Lagrangien transport with a modification of the SYMPHONIE model (Marsaleix *et al.*, 2009). The bacterial communities remained stratified after the numerical simulation of the convective event (Fig. 2), with similar taxonomic compositions as found at ANT station in the AW, LIW and WMDW (Fig. 3). The numerical simulation thus indicated that the pure mixing of the water column was not sufficient to create and maintain the mixed bacterial community observed naturally in the convective cell (SCC). Other factors than the pure hydrological dynamic of the water column were responsible for the resulting composition of the convective prokaryotic communities.

To test this hypothesis, we then used the explanatory power of direct multivariate gradient analysis in order to evaluate the driving forces exerted by environmental parameters on bacterial community distribution before, during and after the convective event (Fig. 4). Under stratified conditions (at the reference station ANT and at the re-stratified SCS station), we observed consistent results with previous

observations under similar conditions in the NW Mediterranean Sea (Ghiglione *et al*., 2008). While the elevated concentrations of nutrient in the WMDW compared with the LIW and AW drove the deep WMDW communities, the intermediate depth communities were driven by the more elevated temperature of the LIW than found in the WMDW and in the AW (Fig. 1 B and C). The surface AW communities were strongly correlated with the elevated DOC and POC surface concentrations accumulated through phytoplankton activities prior to and after the convective mixing. After the convective event, the resilience of the bacterial communities associated with the advection of the LIW was favoured by the rapid return to pre-convective physico-chemical characteristics. To our knowledge, this is the first evidence of resilience of bacterial communities after such a spectacular event and its relation to the rapid return of physico-chemical characteristics back to pre-convective conditions.

During the turbulent mixing, the community structure in the convective cell was highly correlated with POC concentration. In a previous paper, we showed that the convective event observed in this study resulted in a homogenization of the phytoplankton in the convective cell resulted in a homogenization of fresh and highly labile POC (Severin *et al*., 2014). Previous studies showed also an export of massive amount of POM by the convective mixing (Heimbürger *et al*., 2013; Gogou *et al*., 2014). The emergence of a 'convective community' relatively homogeneous on the 0–1000m depth and characterized by a large majority of OTUs usually living in the euphotic zone (Fig. 3) could then be favoured by an homogenization of labile POC. Under stratified conditions, bacterial communities living in surface waters are generally not limited by organic carbon which peaks in the euphotic zone (Van Wambeke *et al*., 2009). The homogenization of labile POC during the convective event may have influenced the selection of bacterial communities normally living in the euphotic zone to form the 'convective community' relatively homogeneous on the 0–1000 m depth and particularly active (see section below). Even if we did not evaluated changes in particle-attached bacterial communities but only in the free-living fraction (<3 μm), previous studies showed that both free-living and particle attached fraction are very connected, with very few particle-specialists and a majority of generalists which colonize and detach rapidly to particles (Ghiglione *et al*., 2009; Ortega-Retuerta *et al*., 2013). Further studies taking into account both particle-attached and free-living fractions may be needed to support our conclusions.

Impact of a deep convection event on the prokaryotic activities

Previous studies in the Sargasso Sea observed an export of labile organic matter in the mesopelagic zone during convective events associated with elevated oxygen utilization rates, thus suggesting carbon remineralization processes (Hansell and Carlson, 2001; Morris *et al*., 2005; Goldberg *et al*., 2009). Here we showed that the convective mixing leads to a stimulation of the PHP with a doubling of the integrated value between 10 and 1500 m despite the strong vertical currents of ± 10 cm s^{-1} prevailing in the convective cell (Durrieu de Madron *et al*., 2013). Even if prokaryotes were exported to unusual pressure in a short period of time, the mixed convective communities possibly took advantages of the labile organic matter exported down to 1500 m. The PHP measured at *in situ* pressure confirm the presence of active piezosensitive prokaryotes at 1500 m depth in the convective cell coming from surface layers. The surface taxa exported down to 1500 m were then still active at unusual pressure. In comparison, the elevated pressure effect ratio (Pe), which is in a similar range to that previously described for the NW Mediterranean Sea (Tamburini *et al*., 2013b), evidences the presence of piezophilic prokaryotes adapted to high pressure in the deep layer of the reference stratified station ANT. In addition, we observed inside the convective cell a decrease of the cell-specific extracellular enzymatic activities in the deep layers, which had an opposite trend to the PHP (Fig. 5). This suggests that the exported organic matter was labile, and may be in the form of monomeric molecules, directly assimilable by prokaryotes, stimulating the secondary production. Additionally to the transfer of surface bacterial taxa down to 1500 m favoured by the export of POM, the composition of this labile DOM exported from the surface seems to mainly favour the development of the typical euphotic *Oceanospirillales* and *Flavobacteriales*. A study in the Adriatic Sea also observed an export of labile DOM, but with a polymeric composition because of an increase of ectoenzyme activities (Azzaro *et al*., 2012). We did not observe any increase of the ectoenzyme activities in our study. Such contradictory results may be explained by the input of fresh labile organic matter associated with the phytoplankton development observed prior to the convection of March 2011 in our study (Severin *et al*., 2014), a phenomena not observed in Azzaro and colleagues (2012).

The influence of the convective event was relatively short since activities returned to usual rates 5 days after the convective mixing, suggesting the depletion of the labile exported DOC. The cessation of the convective vertical currents allowed the advected LIW to cover the area and re-established the stratified bacterial communities between 0 and 500m (Fig. 2). But the remaining mixed bacterial community around 1000 m should then rapidly disappear instead of spreading with the $nWMDW_{mar}$.

Conclusion

Physical oceanographic processes and biogeochemical forcing were necessary to explain the effect of the intense

mixing event on stratified prokaryotic diversity and activities. Despite the importance of convective events on the oceanic circulation and on the regulation of the global biogeochemical cycles, such study is scarce in the literature and reflects the challenge of sampling such event. The strong influence of a convective event on microbial communities, which may be extended to other local physical oceanographic processes such as cascading, upwelling and gyres, reflects the challenges in our ability to understand the role of the prokaryotes in the biogeochemical cycles at a global scale.

Experimental procedures

Sampling sites and procedure

Seawater was collected in the Gulf of Lion with a SBE 32 Carousel of 12 l Niskin bottles equipped with a Seabird 911Plus conductivity-temperature-depth (CTD) profiler deployed from the *RV L'Atalante* at depths between surface and 2000 m (i.e. 10, 50, 100, 350, 500, 1000 and 2000 m) (Fig. 1). The ANTARES station (ANT) sampled on the 2nd of March 2011 was used as a reference away from the convection area. Situated in the centre of the convection area (Severin *et al*., 2014), the SC station was sampled during the convection event on the 4th of March 2011 (SCC) and at the end of the convection event on the 9th of March 2011 (SCS). Biogeochemical parameters including nutrients, as well as chlorophyll and primary production were measured as previously described (Severin *et al*., 2014). DOC was analysed by high temperature catalytic oxidation (HTCO), and dissolved organic nitrogen and phosphorus (DON and DOP, respectively), were analyzed by persulfate wet-oxidation, according to Pujo-Pay and colleagues (2011). POC was analyzed on a CHN Perkin Elmer 2400, while particulate organic nitrogen and phosphorus (PON and POP, respectively), were analysed according to the wet oxidation method, according to Pujo-Pay and colleagues (2011).

Prokaryotic abundance and activities

Prokaryotic abundances were determined by SYBR Green I staining and using a FACSCalibur flow cytometer (Becton Dickinson, San Jose, CA), as previously described (Mével *et al*., 2008).

PHP was measured by ^{3}H-leucine incorporation into proteins using the filtration method (Kirchman, 1993). ^{3}H-leucine (specific activity 155 Ci.mmol^{-1}; Perkin Elmer) was added at final concentration of 20 nM and incubated in the dark for 4 h in triplicate samples from surface waters (0–150 m). For samples from meso- and bathypelagic (>150 m) waters, the final ^{3}H-leucine concentration added was of 10 nM and triplicate samples were incubated for 8h in the dark (calibration curves for 3H-leucine concentrations and incorporation rates depending on depths were previously done). For some deep samples (>1000 m depth), PHP was measured at *in situ* pressure according to Tamburini and colleagues (2002) with the high-pressure methodology described in Tamburini and colleagues (2003) and Boutrif and colleagues (2011). To calculate the PHP, we used the empirical conversion factor of 1.55 ng C. pmol^{-1} of incorporated leucine (Simon and Azam, 1989).

Extracellular enzymatic activities for aminopeptidase, β-glucosidase and lipase were measured using a VICTOR3 spectrofluorometer (Perkin Elmer) after incubations of 4 h (samples from 0 to 150 m) and 8 h (samples deeper than 150 m) at *in situ* temperature with L-leucine-7amido-4-methyl coumarin (LL, 5 μM final), MUF-β-D-glucoside (β-Glc, 0.25 μM final) or MUF-palmitate (Lip, 0.25 μM final), according to Hoppe (1983). These saturated concentrations for LL, β-Glc and Lip and optimized time incubations were determined prior to the extracellular enzymatic activities measurement.

DNA extraction and pyrosequencing

DNA extraction was performed by using the AllPrep mini kit (Qiagen) on 0.2 μm filters (Whatman polycarbonate) after filtration of 2 l of pre-filtered (3 μm) seawater, as previously described (Ghiglione *et al*., 1999). The *V6-V8* hypervariable regions of bacterial and archaeal 16S rRNA genes were amplified using universal primers 926F (5′-AAACTYAAAKGAATTGRCGG-3′) and 1392R (5′-ACGGGCGGTGTGTRC-3′). Tag-encoded FLX amplicons were sequenced using the Roche 454 FLX (Research and Testing Laboratory, Lubbock, TX), producing 300 bp reads.

Sequences were first denoised using AmpliconNoise pipeline, chimera removed with Perseus, then processed and analyzed using the QIIME pipeline, as previously described (Sauret *et al*., 2014). The cleaned sequences were clustered using OTUs at the distance of 0.03, assigned using a modified Greengenes database. In the original Greengenes database, the SAR11 order is mixed with the *Rickettsiales* order. To separate these two groups, the database was modified by extracting the representative sequences identified at a > 97% similarity level as *Rickettsiales*, then aligning these sequences with published full-length 16S rRNA gene sequences defined as SAR11 using MUSCLE, and finally building a tree in QIIME using the FastTree method. We then modified the taxonomy of the representative *Rickettsiales* Greengenes sequences according to their clustering with SAR11 reference sequences. After being assigned with this modified database, our sequences were filtered from mitrochondria and chloroplast OTUs (0.1% and 2.9% of total reads respectively). To enable comparison between samples, sequences were randomly re-sampled from the filtered OTU files to the sample with the fewest sequences for Bacteria (3372) and Archaea (167), by using Mersenne twister PRNG (QIIME 1.8.0). All further analyses were performed on the randomly re-sampled OTU tables.

Because of the small number of Archaea reads, only Bacteria were treated in this study. Further analyses and information on Archaea communities in relation with this study are in the supplementary information (Supporting Information Tables S1 and S3, Figs. S1–S3).

Diversity estimations, similarity between bacterial communities and statistical analysis

Non-parametric species richness estimator Chao1 and ACE were calculated using SPADE software (Chao and Shen, 2003). Rarefaction curves were generated using PAST (PAleontological STatistics v3.01). Simpson, Shannon and Pielou diversity indexes were calculated using PRIMER 6 (PRIMER-E, UK).

Similarity matrices of Bray-Curtis were calculated for each OTU table (Bacteria and Archaea) to compare prokaryotic community structures and were used to build dendrograms by the UPGMA. A similarity profile test (SIMPROF, PRIMER 6) was performed on a null hypothesis that a specific sub-cluster can be recreated by permuting the entry species and samples. The significant branch (SIMPROF, $P < 0.05$) was used as a prerequisite for defining bacterial clusters. One-way analysis of similarity (ANOSIM, PRIMER 6) was performed on the same distance matrix to test the null hypothesis that there was no difference between bacterial communities of different clusters.

Numerical simulation of vertical homogenization of the prokaryotic communities

A model was realized to evaluate the relative contribution of the convective physical mixing on the observed changes in bacterial community structures along the water column. The model was initialized with the stratified bacterial community of the reference station ANT and simulated the convection event of March 2011 at the central station SC. Our simulation used the SYMPHONIE model forced by the real time MERCATOR global model. Based on the real weather observed in February–March 2011, we simulated the convection event encountered during our sampling, including the downward and upward currents coexisting in the convective cell. Here, we hypothesized that Bacteria behave like particles without a sedimentation rate, nor interaction with the biogeochemistry (organic matter assimilation, carbon remineralization or growth rate were not taken into account), thus simulating a pure impact of water mixing only. The Lagrangien transport of the Bacteria (considered here as particles) was simulated by the numerical ocean model SYMPHONIE for deep convection in the Mediterranean Sea (Marsaleix *et al.*, 2009), modified according to Guizien and colleagues (2006) but neglecting the cell motility due to the individual swim. The vertical transport of the Bacteria was directly deduced from the kinetic energy of the vertical currents with a random component in order to simulate the variability of the transport. The hydrology was simulated at the SC station from the 28 February (stratified period prior the convection event) to the 4 March 2011 (end of the convection event) with the products PSY2V4R4 of the ocean model MERCATOR (Drillet *et al.*, 2005) and the data from the European Centre for Medium-Range Weather Forecasts (ECMWF). The resulting model was initialized with the OTU table of the stratified reference station ANT, including the 7 sampling depths. It generated a new OTU table amended with the numerically simulated samples named M10m, M60m, M150m, M350m, M500m, M1000m and M2000m. The resulting simulated convective communities were included in the similarity analysis together with the *in situ* assemblages of stations ANT, SCC and SCS (see above).

Direct multivariate analysis

To investigate the relationships between prokaryotic community structures and environmental parameters, we used canonical correspondence analysis (CCA) multivariate analysis using the software package CANOCO 4.5, as previously described (Berdjeb *et al.*, 2011). Environmental parameters were previously transformed according to their pairwise distributions. Spearman rank pairwise correlations between the transformed environmental variables were used to determine their significance.

Acknowledgements

We are grateful to the crew and officials of R/V *L'Atalante* and to all the scientific and technical staff involved in the CASCADE cruise for their support during sea operations. We are grateful to P. Galand for his advices on the manuscript and to SIROCCO for the modelling. This work was funded by the HERMIONE Project (N° 226354), it was conducted as part of the MERMEX/MISTRALS and is a contribution to IMBER/IGBP program. The authors declare that there are no conflicts of interest.

References

Azzaro, M., La Ferla, R., Maimone, G., Monticelli, L.S., Zaccone, R., and Civitarese, G. (2012) Prokaryotic dynamics and heterotrophic metabolism in a deep convection site of Eastern Mediterranean Sea (the Southern Adriatic Pit). *Cont Shelf Res* **44:** 106–118. doi:10.1016/j.csr.2011.07.011.

Berdjeb, L., Ghiglione, J.-F., and Jacquet, S. (2011) Bottom-up versus top-down control of hypo- and epilimnion free-living bacterial community structures in two neighboring freshwater lakes. *Appl Environ Microbiol* **77:** 3591–3599. doi:10.1128/AEM.02739-10

Boutrif, M., Garel, M., Cottrell, M.T., and Tamburini, C. (2011) Assimilation of marine extracellular polymeric substances by deep-sea prokaryotes in the NW Mediterranean Sea. *Environ Microbiol Rep* **3:** 705–709. doi:10.1111/j.1758-2229.2011.00285.x.

Chao, A. and Shen, T.-J. (2003) Program SPADE *(*Species Prediction and Diversity Estimation*)*. Program and User's Guide [WWW document]. URL http://chao.stat.nthu.edu.tw.

De Corte, D., Yokokawa, T., Varela, M.M., Agogué, H., and Herndl, G.J. (2009) Spatial distribution of Bacteria and Archaea and amoA gene copy numbers throughout the water column of the Eastern Mediterranean Sea. *ISME J* **3:** 147–58. doi:10.1038/ismej.2008.94

Drillet, Y., Bourdallé-Badie, R., Siefridt, L., and Le Provost, C. (2005) Meddies in the Mercator North Atlantic and Mediterranean Sea eddy-resolving model. *J Geophys Res* **110:** C03016. doi:10.1029/2003JC002170.

Ducklow, H. (1999). The bacterial component of the oceanic euphotic zone. *FEMS Microbiol Ecol* **30:** 1–10. doi:10.1016/S0168-6496(99)00031-8.

Durrieu de Madron, X., Houpert, L., Puig, P., Sanchez-Vidal, A., Testor, P., *et al.* (2013) Interaction of dense shelf water cascading and open-sea convection in the northwestern Mediterranean during winter 2012. *Geophys Res Lett* **40:** 1379–1385. doi:10.1002/grl.50331.

Ghiglione, J.F., Philippot, L., Normand, P., Lensi, R., and Potier, P. (1999) Disruption of *narG*, the gene encoding the catalytic subunit of the respiratory nitrate reductase A, also affects nitrite respiration in *Pseudomonas fluorescens* YT101. *J Bacteriol* **181:** 5099–5102. doi:10.1002/grl.50331.

Ghiglione, J.F., Mevel, G., Pujo-Pay, M., Mousseau, L., Lebaron, P., and Goutx, M. (2007) Diel and seasonal variations in abundance, activity, and community structure of particle-attached

and free-living bacteria in NW Mediterranean Sea. *Microb Ecol* **54:** 217–231. doi:10.1007/s00248-006-9189-7.

Ghiglione, J.F., Palacios, C., Marty, J.C., Mével, G., Labrune, C., Conan, P., *et al.* (2008) Role of environmental factors for the vertical distribution (0–1000 m) of marine bacterial communities in the NW Mediterranean Sea. *Biogeosciences* **5:** 1751–1764. doi:10.5194/bg-5-1751-2008.

Ghiglione, J.-F., Conan, P., and Pujo-Pay, M. (2009) Diversity of total and active free-living vs. particle-attached bacteria in the euphotic zone of the NW Mediterranean Sea. *FEMS Microbiol Lett* **299:** 9–21. doi:10.1111/j.1574-6968.2009.01694.x.

Ghiglione, J.F., Galand, P.E., Pommier, T., Pedrós-Alió, C., Maas, E.W., Bakker, K., Bertilson, S.,*et al.* (2012) Pole-to-pole biogeography of surface and deep marine bacterial communities. *Proc Natl Acad Sci USA* **109:** 17633–17638. doi:10.1073/pnas.1208160109.

Gogou, A., Sanchez-Vidal, A., Durrieu de Madron, X., Stavrakakis, S., Calafat, A.M., Stabholz, M., *et al.* (2014) Carbon flux to the deep in three open sites of the Southern European Seas (SES). *J Mar Syst* **129:** 224–233. doi: 10.1016/j.jmarsys.2013.05.013.

Guizien, K., Brochier, T., Duchêne, J.C., Koh, B.S., and Marsaleix, P. (2006) Dispersal of Owenia fusiformis larvae by wind-driven currents: Turbulence, swimming behaviour and mortality in a three-dimensional stochastic model. *Mar Ecol Prog Ser* **311:** 47–66. doi:10.3354/meps311047.

Hansell, D., and Carlson, C. (2001) Biogeochemistry of total organic carbon and nitrogen in the Sargasso Sea: control by convective overturn. *Deep Sea Res Part II Top Stud Oceanogr* **48:** 1649–1667. doi:10.1016/S0967-0645(00)00153-3.

Heimbürger, L.-E., Lavigne, H., Migon, C., D'Ortenzio, F., Estournel, C., Coppola, L., and Miquel, J.-C. (2013) Temporal variability of vertical export flux at the DYFAMED time-series station (Northwestern Mediterranean Sea). *Prog Oceanogr* **119:** 59–67. doi:10.1016/j.pocean.2013.08.005.

Hoppe, H. (1983) Significance of exoenzymatic activities in the ecology of brackish water-measurements by means of methylumbelliferyl-substrates. *Mar Ecol Prog Ser* **11:** 299–308.

Kirchman, D.L. (1993) Leucine incorporation as a measure of biomass production by heterotrophic bacteria. In Handbook of Methods in Aquatic Microbial Ecology. Kemp, P.F., Sherr, B.F., Sherrand, E.B., Cole, J.J. (eds). Lewis Publishers, pp. 509–512.

Marsaleix P., Auclair F., and Estournel C. (2009).Low-order pressure gradient schemes in sigma coordinate models: the seamount test revisited. *Ocean Model* **30:** 169–177. http://dx.doi.org/10.1016/j.ocemod.2009.06.011.

Marshall, J., and Schott, F. (1999) Open ocean convection: observations, theory, and models. *Rev Geophys* **37:** 1–64.

Martín-Cuadrado, A.-B., López-García, P., Alba, J.-C., Moreira, D., Monticelli, L., Strittmatter, A., *et al.* (2007) Metagenomics of the deep Mediterranean, a warm bathypelagic habitat. *PLoS One* **2:** e914. doi:10.1371/journal.pone.0000914.

Martini, S., Nerini, D., and Tamburini, C. (2014) Relation between deep bioluminescence and oceanographic variables: a statistical analysis using time-frequency decompositions. *Prog Oceanogr* **127:** 117–128.

Mével, G., Vernet, M., Goutx, M., Ghiglione, J. (2008) Seasonal to hour variation scales in abundance and production of total and particle-attached bacteria in the open NW Mediterranean Sea (0–1000 m). *Biogeosciences* **5:** 1573–1586.

Millot, C. (1999) Circulation in the Western Mediterranean Sea. *J Mar Syst* **20:** 423–442. doi:10.1016/S0924-7963(98)00078-5.

Morris, R.M., Vergin, K.L., Rappe, M.S., Carlson, C.A., and Giovannoni, S.J. (2005) Temporal and spatial response of bacterioplankton lineages to annual convective overturn at the Bermuda Atlantic Time-series Study site. *Limnol Oceanogr* **50:** 1687–1696.

Najdek, M., Paliaga, P., Šilović, T., Batistić, M., Garić, R., Supić, N., *et al.* (2014) Picoplankton community structure before, during and after convection event in the offshore waters of the Southern Adriatic Sea. *Biogeosciences* **11:** 2645–2659. doi:10.5194/bg-11-2645-2014.

Ortega-Retuerta, E., Joux, F., Jeffrey, W.H., and Ghiglione J.F. (2013) Spatial variability of particle-attached and free-living bacterial diversity in surface waters from the Mackenzie River to the Beaufort Sea (Canadian Arctic). *Biogeosciences* **10:** 2747–2759. doi:10.5194/bg-10-2747-2013.

Pommier, T., Neal, P., Gasol, J., Coll, M., Acinas, S., and Pedrós-Alió, C. (2010) Spatial patterns of bacterial richness and evenness in the NW Mediterranean Sea explored by pyrosequencing of the 16S rRNA. *Aquat Microb Ecol* **61:** 221–233. doi:10.3354/ame01484.

Pujo-Pay, M., Conan, P., Oriol, L., Cornet-Barthaux, V., Falco, C., Ghiglione, J.-F., Goyet, C., Moutin, T., Prieur, L. (2011) Integrated survey of elemental stoichiometry (C, N, P) from the western to eastern Mediterranean Sea. *Biogeosciences* **8:** 883–899. doi:10.5194/bg-8-883-2011.

Pulido-Villena, E., Ghiglione, J.-F., Ortega-Retuerta, E., Van Wambeke, F., and Zohary, T. (2012) Heterotrophic bacteria in the pelagic realm of the mediterranean sea, In Life in the Mediterranean Sea: A Look at Habitat Changes. Stambler, N. (ed). Nova Science Publishers, pp. 227–265.

Rodríguez-Blanco, A., Ghiglione, J.-F., Catala, P., Casamayor, E.O., and Lebaron, P. (2009) Spatial comparison of total vs. active bacterial populations by coupling genetic fingerprinting and clone library analyses in the NW Mediterranean Sea. *FEMS Microbiol Ecol* **67:** 30–42. doi:10.1111/j.1574-6941.2008.00591.x.

Santinelli, C., Nannicini, L., and Seritti, A. (2010) DOC dynamics in the meso and bathypelagic layers of the Mediterranean Sea. *Deep Sea Res Part II Top Stud Oceanogr* **57:** 1446–1459. doi:10.1016/j.dsr2.2010.02.014.

Sauret, C., Séverin, T., Vétion, G., Guigue, C., Goutx, M., Pujo-Pay, M., Conan, P., Fagervold, S.K., Ghiglione, J.-F. (2014) "Rare biosphere" bacteria as key phenanthrene degraders in coastal seawaters. *Environ Pollut* **194:** 246–253.

Schott, F., and Leaman, K. (1991) Observations with moored acoustic Doppler current profilers in the convection regime in the Golfe du Lion. *J Phys Oceanogr* **21:** 558–574.

Send, U., and Marshall, J. (1995) Integral effects of deep convection. *J Phys Oceanogr* **25:** 855–872.

Simon, M., and Azam, F. (1989) Protein content and protein synthesis rates of planktonic marine bacteria. *Mar Ecol Prog Ser* **51:** 201–203.

Severin, T., Conan, P., Durrieu De Madron, X., Houpert, L., Oliver, M.J., Oriol, L., Caparros, J., Ghiglione, J.F., Pujo-Pay, M. (2014) Impact of open-ocean convection on nutrient, phytoplankton biomass and activity. *Deep Sea Res Part I Oceanogr Res Pap* **94:** 62–71.

Stabholz, M., Durrieu de Madron, X., Canals, M., Khripounoff, A., Taupier-Letage, I., Testor, P., *et al.* (2013) Impact of open-ocean convection on particle fluxes and sediment dynamics in the deep margin of the Gulf of Lions. *Biogeosciences* **10:** 1097–1116. doi:10.5194/bg-10-1097-2013.

Sunagawa, S., Coelho, L.P., Chaffron, S., Kultima, J.R., Labadie, K., Salazar, G., *et al.* (2015) Structure and function of the global ocean microbiome. *Science* **348:** 1261359. doi: 10.1126/science.1261359.

Tamburini, C., Garcin, J., Ragot, M., and Bianchi, A. (2002) Biopolymer hydrolysis and bacterial production under ambient hydrostatic pressure through a 2000 m water column in the NW Mediterranean. *Deep Sea Res Part II Top Stud Oceanogr* **49:** 2109–2123. doi:http://dx.doi.org/10.1016/S0967-0645(02)00030-9.

Tamburini, C., Garcin, J., and Bianchi, A. (2003) Role of deep-sea bacteria in organic matter mineralization and adaptation to hydrostatic pressure conditions in the NW Mediterranean Sea. *Aquat Microb Ecol* **32:** 209–218. doi:10.3354/ame032209.

Tamburini, C., Garel, M., Al Ali, B., Mérigot, B., Kriwy, P., Charrière, B., and Budillon, G. (2009) Distribution and activity of Bacteria and Archaea in the different water masses of the Tyrrhenian Sea. *Deep Sea Res Part II Top Stud Oceanogr* **56:** 700–712. doi:10.1016/j.dsr2.2008.07.021.

Tamburini, C., Canals, M., Durrieu de Madron, X., Houpert, L., Lefèvre, D., Martini, S., *et al.* (2013a) Deep-sea bioluminescence blooms after dense water formation at the ocean surface. *PLoS One* **8:** e67523. doi:10.1371/journal.pone.0067523.

Tamburini, C., Boutrif, M., Garel, M., Colwell, R.R., and Deming, J.W. (2013b) Prokaryotic responses to hydrostatic pressure in the ocean–a review. *Environ Microbiol* **15:** 1262–1274. doi:10.1111/1462-2920.12084.

Tanaka, T., and Rassoulzadegan, F. (2004) Vertical and seasonal variations of bacterial abundance and production in the mesopelagic layer of the NW Mediterranean Sea: bottom-up and top-down controls. *Deep Sea Res Part I Oceanogr Res Pap* **51:** 531–544. doi:10.1016/j.dsr.2003.12.001.

Ter Braak, C.J.F., and Šmilauer, P. (2002) *CANOCO Reference Manual and CanoDraw for Windows User's Guide: Software for Canonical Community Ordination (version 4.5)*. Ithaca NY, USA: Microcomputer Power.

Testor, P., and Gascard, J.-C. (2006) Post-convection spreading phase in the Northwestern Mediterranean Sea. *Deep Sea Res. Part I Oceanogr Res Pap* **53:** 869–893. doi: 10.1016/j.dsr.2006.02.004.

Van Wambeke, F., Ghiglione, J.F., Nedoma, J., Mével, G., Raimbault, P. (2009) Bottom up effects on bacterioplankton growth and composition during summer-autumn transition in the open NW Mediterranean Sea. *Biogeosciences* **6:** 705–720. doi:10.5194/bg-10-2747-2013.

Supporting information

Additional Supporting Information may be found in the online version of this article at the publisher's web-site:

Table S1. Number of OTUs and Chao1, Pielou, Shannon and Simpson diversity indexes at 0.03 level of clustering for re-sampled Bacteria (3372 reads) and Archaea (162 reads) OTU table at stations ANT (the stratified reference station), SCC (the convective station) and SCS (the stratified station) sampled at different depths.

Table S2. Covariables and representative variable selected for the CCAs analyses at each station: ANT (the stratified reference station), SCC (the convective station), SCS (the restratified station).

Table S3. Summary of results from the canonical correspondence analyses (CCAs) of the Bacteria and Archaea community structures at stations ANT (the stratified reference station), SCC (the convective station) and SCS (the restratified station) when constrained by the environmental variables described in Fig. 4 for Bacteria and Fig. S3 for Archaea.

Fig. S1. Unweighted-pair group method with arithmetic mean (UPGMA) dendrograms based on Bray-Curtis similarities of 16S rRNA gene reads of Archaea from ANT (the stratified reference station), SCC (the convective station) and SCS (the restratified station) sampled at different depths. Results of ANOSIM tests (R) are indicated at the main nodes and indicate that at the stratified stations (ANT and SCS) Archaea community of each water mass (AW, LIW and WMDW, indicated by rectangles) clustered together and independently of the station like Bacteria communities (Fig. 2), highlighting a strong resilience of the archeal communities in stratified conditions. Archaeal community was also homogeneous throughout the 0–1500 m mixed water layer (SCC10m to SCC1000m) like the bacterial community during the convection, and differed for the deepest sample SCC2000m located below the mixing zone.

Fig. S2. Archaeal taxonomic distribution (Phylum_Class_Order_Family) for OTUs that occurred more than 2 times ($>$1% of randomly re-sampled 167 sequences reads at a clustering distance of 0.03) in the OTU table. The remaining sequences are grouped in «other». Taxonomy not assigned, NA. Samples from the same water masses (AW, LIW and WMDW) are indicated by rectangles. At the stratified stations (ANT and SCS), Marine group II Euryarchaeota dominated at $\sim$60% the surface AW, and Marine group I Thaumarchaeota dominated the LIW (88%) and WMDW (83%). The convective community (SCC) was dominated by both Marine group I (50%) and II (50%), a mix of surface and deep OTUs like for Bacteria community structure.

Fig. S3. Canonical correspondence analysis (CCAs) of archaeal community structure at each sampled station: ANT (A; stratified reference station), SCC (B; convection station), SCS (C; restratified station). Arrows point in the direction of increasing values of each variable. The length of the arrows represents degree of correlation with the 2 first axes. NO_3+NO_2: nitrate + nitrite. DOP: dissolved organic phosphorus. DON: dissolved organic nitrogen. PON: particulate organic nitrogen. Chla: chlorophyll a. Like for Bacteria communities (Fig. 4), in stratified (ANT) and restratified (SCS) stations, communities from LIW and WMDW ($>$ 350 and 100 m for ANT and SCS, respectively), are driven by nutrient, while the surface communities in AW is driven by organic matter and higher temperature than the deep one. During the convection (SCC), the Archaea community from 10 to 1000 m is driven by organic matter, chlorophyll *a* and more elevated temperature than at 2000 m.